ORIGINAL ARTICLE

Modified Variable Droop Control Strategy for Improved Primary Frequency Response in Wind Turbine Generators using ROCOF

Joseph Shin[1] · Suhyeon Han[1] · Sejin Lee[1] · Youngsung Kwon[1]

Abstract

Frequency control is one of the challenges in wind turbine generation. One frequency control method used by wind turbine generators (WTGs) is droop control. In the droop control method, various strategies have been devised to continually update the droop gain to suit the current situation. This study proposes a modified droop control method that uses the advantages of two variable droop control strategies based on the system frequency deviation: the rate of change of frequency (ROCOF)-based method and the frequency-dependent method. Moreover, limits were set in the droop gain value based on the rotor speed. The proposed ROCOF-based frequency-dependent droop control strategy aims at maximizing the frequency nadir improvement with a quick primary frequency response reaction time while preventing secondary frequency drop or stall of the turbines. These improvements can be used to increase wind penetration in the system, allowing for the reduction of fossil fuel use. The frequency regulation performance of the proposed droop control strategy was compared with other droop control methods in the MATLAB/Simulink environment using a doubly fed induction generator (DFIG) WTG model based on the National Renewable Energy Laboratory Fatigue, Aerodynamics, Structures, and Turbulence model.

Keywords Doubly fed induction generator · Frequency nadir · Rate of change of frequency · Droop gain

1 Introduction

When the importance of renewable energy is greater than ever, wind power generation is receiving increasing attention because of its eco-friendliness and efficiency in space [1–4].

Among the various types of wind turbine generators (WTGs) on the market, doubly-fed induction generators (DFIGs) are among the most widely used because of their efficiency and flexibility in operating speed [5]. DFIGs, also known as type 3 wind turbine generators, operate by employing an AC/DC/AC converter in the rotor circuit, allowing for maximized wind power extraction and lowered mechanical

stresses [6]. Owing to its advantages and widespread use, the DFIG model was used for the operations in this study.

However, the use of wind power generation and DFIGs also presents challenges. Unlike other conventional methods of generation, WTGs mainly use induction generators, which decouple the rotational speed from the grid frequency. In turn, they do not contribute to grid inertia, which is problematic in terms of frequency control, which is the process of maintaining a steady frequency in the grid with minimal fluctuations [7]. In a generator, when the consumed power exceeds the generation power, the system frequency decreases. The opposite applies, where the system frequency increases when the generated power exceeds the consumed power [8]. Thus, as wind penetration in an electrical grid increases, its tendency to deviate from its operating frequency also increases during a system event [9]. Various frequency control operations exist to maintain the frequency of the grid within the operating range.

The first method is to supply energy from the energy storage system (ESS) connected to the wind turbine when frequency fluctuations occur [10]. An ESS is a large-scale energy storage system introduced to supplement the fluctuating power generation output of wind turbines and

✉ Youngsung Kwon
   youngsung.kwon@handong.edu

   Joseph Shin
   joeshin3956@hanyang.ac.kr

   Suhyeon Han
   21900785@handong.ac.kr

   Sejin Lee
   mecarry@handong.ac.kr

1 Department of Mechanical and Control Engineering, Handong Global University, Pohang-Si, Korea

maintain a stable frequency of the power system. When a frequency drop occurs, the ESS can stably adjust the frequency of the power system by transferring stored energy to the grid [11]. However, ESS has the disadvantage of a high investment cost, considering the complexity of communication interaction and economic cost [12].

Second, deloading control is an operation in which the WTG is operated at speeds at which the generating efficiency is suboptimal, resulting in reserve power to stabilize the frequency in the case of a grid event. This deloading operation is achieved by either lowering the speed through pitch control or increasing it with over-speed control [13, 14]. Pitch control is a method of adjusting the angle at which the turbine blades are positioned relatively to the wind to limit the amount of wind energy transferred to the rotors [15–17]. Overspeeding occurs when the WTG operates at a rotational speed faster than its maximum power point (MPP). The reserve power obtained by pitch control and overspeeding is later used to regulate the frequency during the system event. Although effective in frequency stabilization, running wind turbines at a suboptimal efficiency results in a significant loss of annual wind energy. Moreover, the frequent activation of pitch control in a WTG increases the mechanical stress within the unit.

A frequency control method that mitigates these drawbacks is droop control. Droop control is a method that uses the rotational energy stored within the generators and thus does not require the WTG to be operated at a suboptimal power, resulting in less energy loss. Droop control operates by utilizing the droop characteristics of generators to manipulate the difference between the input mechanical power and output electrical power, changing the electrical frequency [18, 19]. The magnitude of the frequency change that occurs during this process is determined by the droop control gain. Thus, various strategies have been employed to adjust the value of the droop gain to achieve optimal frequency control.

The optimal droop gain at a given time varies depending on several factors. One of these factors is the turbine's rotor speed, for the rotational speed is what determines the available mechanical energy within the WTG [20, 21]. However, this method does not consider the magnitude of the frequency deviation in the system. The system frequency at a given time determines how much frequency regulation should occur to mitigate frequency fluctuations, which is an important factor for efficient frequency control.

Therefore, this study focuses on two fundamental strategies for frequency-deviation-related droop gain adjustment: rate of change of frequency (ROCOF)-based droop gain and frequency-dependent droop gain, each with its advantages and disadvantages.

ROCOF-based droop control, which has a quick reaction time during the primary frequency response, is highly sensitive to measurement errors and frequency noise, as ROCOF is the derivative of the frequency deviation [14].

The frequency-dependent droop control is effective at improving the frequency nadir, as it regulates the frequency based on the deviation in frequency [20]. However, it is slower in terms of reaction time than the ROCOF-based droop control method, as its droop gain is a function of the frequency deviation and not its derivative.

Therefore, this study proposes an ROCOF-based frequency dependent (RFD) droop control that retains the individual advantages of the two previous droop control methods. The aim is to couple the ROCOF-based droop control method's quick reaction time with the frequency nadir (FN) improvement of the frequency-dependent droop control gain by selecting the droop gain as a function of both the ROCOF and frequency deviation. Furthermore, high and low limits were set in the variable droop gain based on the rotor speed, disabling the turbine from contributing beyond its kinetic energy margin, thus preventing a secondary frequency drop and turbine stalling. With these improvements, the previous challenges with frequency regulation through WTGs were mitigated, potentially allowing for higher wind penetration in the system. The performance of this method was compared to its original counterparts of the ROCOF-based and frequency-based droop control schemes within the MATLAB Simulink environment using the NREL's Fatigue, Aerodynamics, Structures, and Turbulence (FAST) wind turbine models [6].

The results show that the RFD method can successfully retain the frequency nadir improvement of the FD method, with approximately 5.07%-8.25% higher FN improvement than the ROCOF-based method, while achieving a quick reaction time of approximately 39.58% faster than that of the FD method.

The remainder of this paper is organized as follows. Section 2 explains the generation and control operations of WTGs, specifically the DFIGs. Section 3 introduces the concept and various droop control strategies, including the proposed RFD droop control method used in this study. Section 4 contains the specifications of the power system model designed for droop control simulation. Section 5 presents the simulation results for each scenario. Finally, Sect. 6 concludes the paper.

2 Modeling of Doubly Fed Induction Generator

In this section, we used a 1.5 MW FAST DFIG model provided by NREL [6]. The WTG includes the turbine aerodynamics, drivetrain model, DFIG, and tower effect. In this

study, we propose an optimal droop-control strategy for primary frequency support.

2.1 Wind Turbine Aerodynamics

Wind turbines convert aerodynamic energy into mechanical energy using blades. Subsequently, the rotational speed is quickly converted through the gearbox, and mechanical energy is transmitted to the generator to generate electrical energy [22, 23]. The mechanical power (P_m) delivered to the DFIG is expressed as [24, 25]

$$P_m = \frac{1}{2}\rho A v_w^3 Cp(\lambda, \beta) \tag{1}$$

$$\lambda = \frac{\omega_r R}{v_w} \tag{2}$$

where ρ is the air density, A is the rotor sweep area, v_w is the wind speed, Cp is the power coefficient, λ is the tip- speed ratio, β is the pitch angle, ω_r is the rotor speed, and R is the blade radius.

The output power can be adjusted by adjusting Cp. Cp is determined by the tip-speed ratio and pitch angle [14, 26].

2.2 Pitch Controller

Pitch control is a process in which the turbine blades of a WTG are angled such that only a fraction of the total energy is captured by the wind turbine. This is a process aimed at controlling the rotor speed and mechanical power of the turbine to protect the rotor from damage owing to spinning at excessively high speeds.

The pitch determines the mechanical output power of the wind turbine based on Eq. (1). A pitch controller adjusts this pitch value based on how the user aims to control rotor speed and output power.

The pitch controller usually uses a non-linear pitch servo. The servo is used for proper positioning of the blade. In the closed loop, the servo is modeled as a first-order delay system with a time constant (τ_c) as follows [17]:

$$\frac{d\beta}{dt} = -\frac{1}{\tau_c}\beta + \frac{1}{\tau_c}\beta_{ref} \tag{3}$$

where β is the pitch angle, τ_c is the time constant, β_{ref} is the reference pitch angle value.

The pitch angle is subject to:

$$\beta_{min} \leq \beta \leq \beta_{max} \tag{4}$$

where β_{min} is the minimum pitch angle and β_{max} is the maximum pitch angle. The values of β_{min} and β_{max} represent the physical limitations of the pitching of the rotor blade.
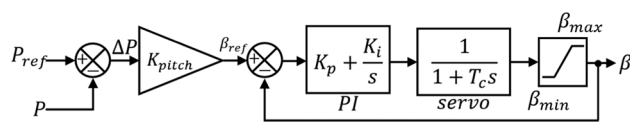

Fig. 1 Block Diagram of Pitch Controller

In this study, a simple pitch controller was used as shown in Fig. 1. The pitch controller calculates the pitch angle at which the output power becomes the reference power. That is, according to Eq. (1), the pitch angle is adjusted through the pitch controller to obtain the output desired by the user. In Fig. 1, when the reference power and current power are input to the wind turbine, ΔP is the output. ΔP is multiplied by the pitch controller gain and the reference pitch angle is derived. The value obtained by subtracting the current pitch angle from the reference pitch angle goes through the PI controller and servo transfer function. The servo transfer function is taken from the nonlinear model in Eq. (3). Finally, to prevent damage to the blade, the pitch angle is limited, and the pitch angle is derived as the result. This is illustrated as the following:

Where P_{ref} is the reference power value; P is the current output power; β_{ref} is the reference pitch angle; and K_p and K_i are the proportional and integral constants of the PI controller; T_c is a time constant of the servo, respectively.

2.3 Doubly Fed Induction Generator

In this study, a DFIG model was used for the generator part of the simulation, making it a type 3 wind turbine generator. Their wide range of operation in wind speeds and high efficiency make them more viable than type 1 or 2 wind turbine generators. Additionally, they are more affordable than permanent magnet synchronous generators (PMSGs), also known as type 4 wind turbine generators, because PMSGs require expensive high-capacity converters rated for the entire output power, making DFIGs currently the most popular turbine in the market.

In DFIGs, there is a specific relationship between the change in rotor speed and mechanical/electrical torque. For this study, the variable-speed rigid drive train representation was used, enabling the change in the generator rotor speed to be calculated using the following equation:

$$\frac{dw_r}{dt} = \frac{1}{2H}\left(T_m - T_e\right) \tag{5}$$

where w_r is the generator rotor speed [rad/s], T_m is the mechanical torque [pu], T_e is the electrical torque, and H is the inertia constant.

3 Droop Control

In this section, the concept of droop gain control is introduced, followed by an explanation of the two existing variable droop control methods. There is then a technical description of the modified approach to droop control proposed in this study.

3.1 Concept of Droop Gain Control

Primary droop controllers are designed to prevent frequency drop by using the system frequency deviation.

The droop parameter, %R, is defined as follows:

$$\%R = \frac{\Delta f}{\Delta P}100 \tag{6}$$

where Δf is the frequency deviation [pu] and ΔP is the incremental change in power [pu]. ΔP is the additional amount of power that wind power supplies to the grid to compensate for frequency deviation.

Equation (6) shows that the smaller the value of the droop parameter, the greater the wind power supply according to the frequency change. That is, the smaller the value of the droop parameter, the more energy the wind power supplies depending on the grid frequency deviation.

The small droop parameter can lead to unstable power generation due to the excessive energy contribution of WTG, while a large droop parameter limits the ability to stabilize the frequency due to a small contribution to the energy supply. Therefore, it is important to set appropriate droop parameter values.

3.2 Fixed Droop Control

The fixed droop operation leaves the droop gain at a constant value with no adjustments during generation. Although it is the simplest form of droop gain selection, it lacks the capability to change the droop gain value based on varying conditions. To compensate for this drawback, variable droop operations have been researched, where the droop value is constantly optimized based on changing conditions [20, 21].

One of the conditions considered by many variable droop strategies is rotor speed. The rotor speed prevents the over contribution of the droop control, allowing stable operation. However, a flaw of this method is that because only the rotational speed of the turbine is considered, the frequency deviations are unaccounted for.

Thus, another variable condition considered by the variable droop control strategy is frequency deviation. These operations adjust the droop gain value based on how much a system event causes the frequency to deviate from its nominal value, and various methods which utilize this concept.

3.3 ROCOF-based Droop Control

One form of frequency-deviation-related variable droop control is using the ROCOF to adjust droop gain. ROCOF is the derivative of the system frequency and can be used in numerous ways to calculate the adjusted droop gain value. One of these methods is to set the droop control gain as a linear function of ROCOF [21]:

This strategy enables the WTG to adaptively adjust to the disturbances in the frequency, owing to the positive relationship between the ROCOF and system frequency disturbance. Moreover, ROCOF has a large value in the initial stage of an event, making the value increase of the droop gain quicker than most other variable droop control methods, resulting in a quicker reaction time [27].

However, because the droop gain is a function of ROCOF, a derivative of the frequency error, this strategy is highly sensitive to the measurement error and noise of the frequency. Moreover, ROCOF reaches a value of zero during the frequency nadir, which limits its ability to mitigate frequency deviation when used by itself.

3.4 Frequency-dependent Droop Control

Another method of variable droop control related to the frequency deviation is the frequency-dependent droop-gain strategy. Here, the droop gain, expressed as $G(f_{sys})$, is set to depend on the frequency deviation and can be represented as follows [20]:

$$G(f_{sys}) = C_{FD} \times \Delta f + \frac{1}{R_{con}} \tag{7}$$

where f_{sys} is the system frequency, $G(f_{sys})$ is the droop gain, $1/R_{con}$ is the droop gain of conventional fixed droop schemes, and C_{FD} is the frequency regulation factor, which is a constant that adjusts the performance to improve the frequency regulation capability.

Because the frequency-dependent droop gain method varies its droop gain based on the system frequency deviation, the frequency fluctuations of the electric power system are effectively reduced. However, the frequency-dependent droop control strategy lacks the quick reaction time of the ROCOF-based method because the droop gain is a function of the frequency deviation and not the ROCOF. A comparison of some of the attributes of both the ROCOF-based method and frequency-dependent method is given in Table 1.

3.5 RFD Droop Control

The existing FD droop control has a good performance on PFR, but the response speed is not faster than that of the

Table 1 Comparison of ROCOF-based Droop Control and Frequency-dependent Droop Control

Droop control method	Frequency nadir reduction	Reaction time	Noise sensitivity
ROCOF-based	Moderate	Fast	High
Frequency-dependent	Effective	Slow	Moderate

ROCOF droop control. The ROCOF droop control has a faster PFR speed than the FD droop control; however, the FN improvement ability is not as good as that of FD droop control.

The RFD droop control gain is designed as shown in Fig. 2, and the droop power output can be expressed as:

$$G_{RFD} = C_{RFD} \times \Delta f + \frac{1}{R_\omega} \tag{8}$$

$$C_{RFD} = K_{RFD} \times \frac{df}{dt} + C_{FD} \tag{9}$$

where G_{RFD} is the RFD droop gain, C_{RFD} is the RFD droop control gain, K_{RFD} is a constant multiplied by ROCOF, C_{FD} is the frequency regulation factor of the FD droop control, and R_ω is the proportional control parameter determined by the rotor speed.

The RFD droop control adds the characteristics of the ROCOF to the FD droop control strategy. Equation (8) and (9) are expressions of RFD droop control as formulas. In the existing FD droop control strategy, the frequency regulation factor, C_{FD}, has a fixed value. The frequency regulation factor of the RFD droop control, C_{RFD}, adjusts the gain to increase based on ROCOF. Consequently, an effective FN improvement and fast PFR can be achieved by adding the ROCOF feature to the FD droop control strategy. Furthermore, the RFD droop control does not require excessive computation because it only adds the characteristics of the ROCOF to the existing FD strategy. Therefore, it is expected that it can be performed quickly when performing feedback control.

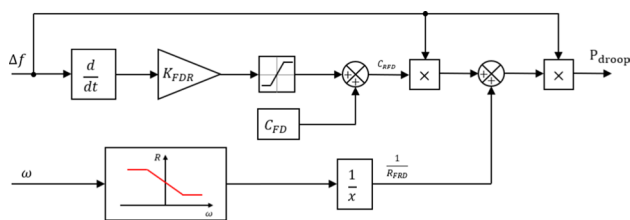The limit in Fig. 2 makes the value of df/dt less than zero and limits the WTG from having a droop gain that is overly large. The ROCOF signal changes from negative to positive at the lowest point of frequency drop which causes unstable droop control at the inflection point of the frequency. Because this hinders the ability to regulate the frequency, the size of df/dt entering the RFD controller is limited to $df/dt < 0$.

The grid codes of various countries limit the value of the droop parameter between 3 and 6% for stable grid [5]. Therefore, in this study, the maximum value of the droop parameter (R_{max}) is set to 6% and the minimum value of the droop parameter (R_{min}) to 3%.

R_ω of Eq. (8) is determined as shown in Fig. 3. Referring to the fact that the minimum operating rotor speed range of DFIG is 0.7 pu [14], R_ω is limited to R_{max} when the rotor speed rotates below 0.75 pu. This strategy avoids the secondary frequency drop that occurs when droop control provides PFR at low-speed rotation.

When the wind speed is high, the wind turbine has more rotational energy, which allows it to provide more active power [28]. However, if a lot of rotational energy is supplied as active power, a secondary frequency drop occurs because energy is consumed in the process of returning to the original rotational speed again [11, 30]. Therefore, wind turbines should not provide excessive energy when the wind speed is high.

Thus, when the wind speed is high, R_ω should be limited such that the PFR does not become excessively large, even if the kinetic energy is large. Therefore, when setting R_{min} at a rotor speed ω_2, the value should not be less than 3%.

4 Modeling of Power System Simulation

To check the performance of the RFD proposed in this study, the following power system was designed. Referring to [20, 29], and [30], a wind farm consisting of eight thermal power plants, static load, motor, and DFIG was designed. The designed power system is shown in Fig. 4.

In a situation where a stable frequency was maintained, the ability to adjust the frequency of wind power generation was analyzed when one 55 MW synchronous
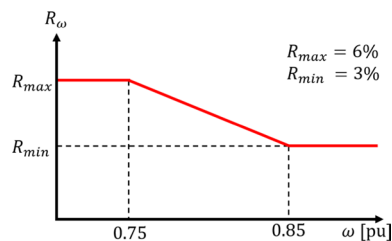
Fig. 2 RFD Droop Control Scheme Block Diagram

Fig. 3 Setting of R_ω Based on Rotor Speed
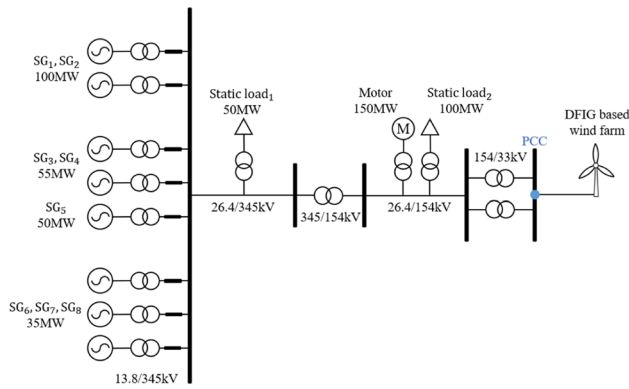
Fig. 4 Model of Power System
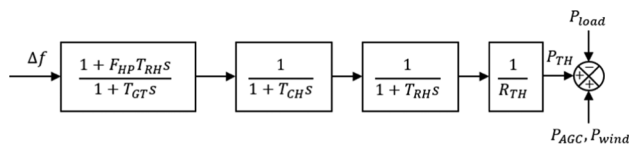
Fig. 5 4 MW Synchronous Generator Governor Model

Table 2 Parameters of Thermal Generator

T_{CH}	T_{GT}	F_{HP}	T_{RH}	R_{TH}
0.3	0.2	0.3	7.0	0.05

generator (SG) was suddenly disconnected from the system owing to an accident in 70 s.

In Sect. 5, droop control performance based on (1) wind penetration and (2) wind speed was analyzed. The wind penetration levels were calculated using Eq. (10) in [14].

$$Wind\ penetration\ level\ (capacity) = \frac{P_{installed.wind}}{P_{max,load}} \quad (10)$$

For the synchronous generator model, refer to [29]. When the frequency deviation entered the input of the steam turbine of the synchronous generator, the corresponding P_{TH} was the output. The synchronous generator model and parameters used are shown in Fig. 5 and Table 2.

T_{CH} is the steam turbine time constant of the main inlet and steam chest, T_{GT} is the speed governor time constant of the thermal unit, F_{HP} is the steam turbine reheat time, T_{RH} is the reheat time constant, and R_{TH} is the droop gain of steam turbine.

Table 3 FN improvement relative to No-droop control method (%)

Method	Case 1	Case 2	Case 3	Case 4	Case 5
Fixed gain (20)	6.58	13.04	18.26	17.96	17.69
ROCOF method	6.95	13.49	18.68	18.41	17.86
FD method	9.41	17.36	22.85	22.92	21.87
RFD (proposed)	12.02	21.00	26.93	23.48	25.51

Table 4 Reaction times of each droop control method (s)

Method	Case 1	Case 2	Case 3	Case 4	Case 5
Fixed gain (20)	0.44	0.45	0.54	0.52	0.46
ROCOF method	0.32	0.37	0.44	0.45	0.40
FD method	0.48	0.47	0.51	0.52	0.51
RFD (proposed)	0.29	0.35	0.42	0.39	0.42

5 Results

In this section, simulations were conducted to verify the performance of the RFD droop control strategy proposed in this study. Droop control depends highly on wind penetration and speed. Wind penetration determines the inertial constant and magnitude of the PFR. The wind speed determines the rotational energy available to the DFIG.

There are a total of five cases. Cases 1 to 3 compare the results based on wind penetration, and Cases 4 to 5 compare the results based on wind speed. This study analyzed the degree of FN improvement and PFR speed, which are displayed in Tables 3 and 4.

The FN improvement was calculated by comparing the frequency deviation of the no-droop control method with the frequency deviation of each droop control method. The value was derived by subtracting the frequency deviation of each droop control method from the no-droop control method, then dividing that value by the frequency deviation magnitude of the no-droop control method. This allowed visualization of how much the presence of each droop control method improved the FN.

The PFR speed was calculated by measuring the time in which the output power of each droop control method reached maximum value during the simulation, then subtracting 70 s from that time. This was because the SG trip was given at the 70 s mark, meaning the calculated value, called the reaction time, represents the time from which the SG trip was given to the time when the power output reached its maximum value.

5.1 Wind Penetration

Wind penetration refers to the percentage of the total power output of a power plant in which WTGs are generated. The level of wind penetration has a significant effect on the frequency regulation of a system because differences in wind penetration result in different degrees of inertia constants and primary frequency control capabilities. For Cases 1 to 3, the wind speed was set at a fixed value of 7 m/s, while the wind penetration was set as 8.1, 16.3, and 23.2%, respectively. With these parameters, the frequency and WTG output power were observed to investigate the performance of the different droop control methods in conditions with different wind penetration values. The simulations of Cases 1, 2, and 3 are displayed in Figs. 6, 7 and 8, respectively.

5.1.1 Case 1: Wind Speed = 7 m/s, Penetration = 8.1%

In Fig. 6a, the frequency of the wind turbine generator can be observed under five different droop control methods. With the system event of the SG trip at the 70 s mark, all five methods show a sudden dip in frequency, followed by a frequency increase, which recovers the frequency of the system over a period.

In Fig. 6a, it is observed that the RFD method has the highest FN improvement, 2.61% greater than that of the FD scheme, which has the second lowest FN improvement, and 5.44% greater than that of the fixed-gain droop scheme, which has the lowest FN improvement out of the droop control schemes (except for the no-droop control scheme).

Figure 6b shows the total output power of the wind turbine generator under five different droop control schemes. Upon the SG trip at 70 s, all methods except for the no-droop control scheme show an abrupt rise in output power, followed by a dip and recovery to the steady-state power level. To compare how quickly a droop control method can react to a system event, the reaction time was analyzed in this section. The reaction time refers to the time required for the output power to reach its highest value when the SG trip occurred at 70 s.

Upon close inspection, it can be observed that the RFD and ROCOF methods show similar reaction times of 0.29 s and 0.32 s respectively, being quicker than the FD's reaction time by over 33%.

It can be observed from these results that any form of droop-control method gives an improved FN value. Among the different droop control methods, the proposed RFD.
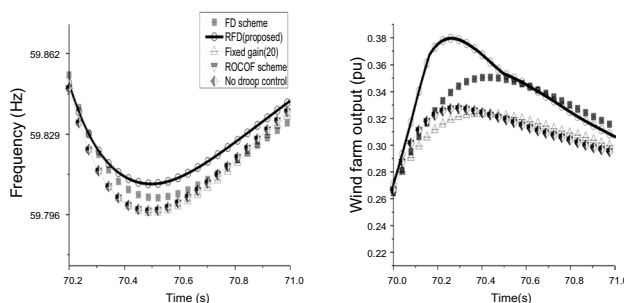
scheme shows the smallest frequency deviation and fastest reaction time. This is because of the RFD method's design of combining the FD method's high FN and ROCOF method's quick reaction time, thus showing the advantages of both methods, evident by the fact that the FD method
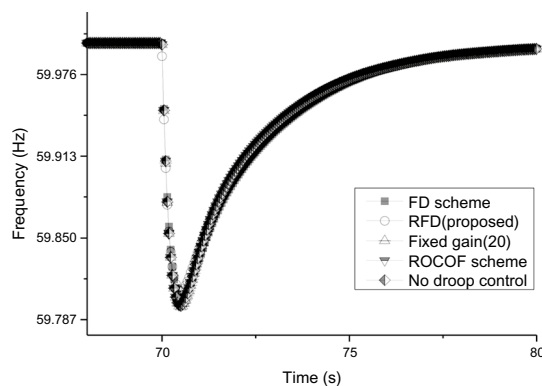
(a) System frequency
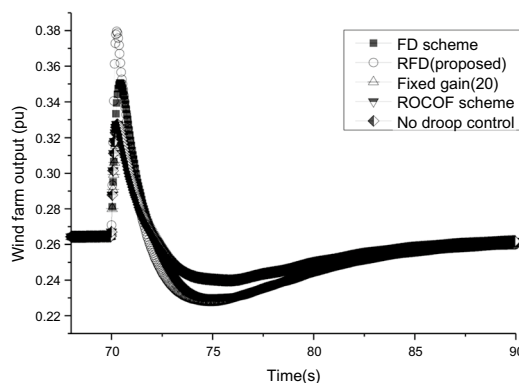
(b) Power output

(c) Close-up versions of the system frequency (left) and power output (right)

Fig. 6 Simulation results for Case 1

shows the second highest FN, and the ROCOF method shows the second quickest reaction time.

5.1.2 Case 2: Wind Speed = 7 m/s, Penetration = 16.3%

For Case 2, all simulation parameters were identically set to Case 1 except for the wind penetration, which increased
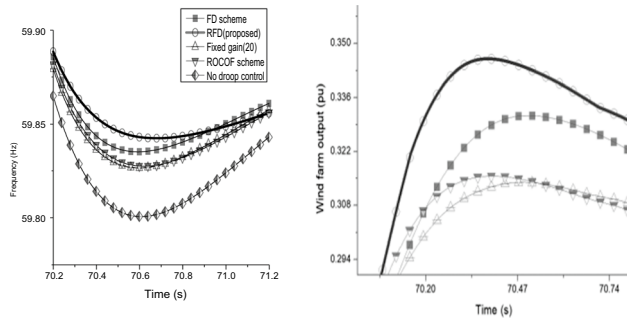
Fig. 7 Close-up versions of system frequency (left) and power output (right) for Case 2
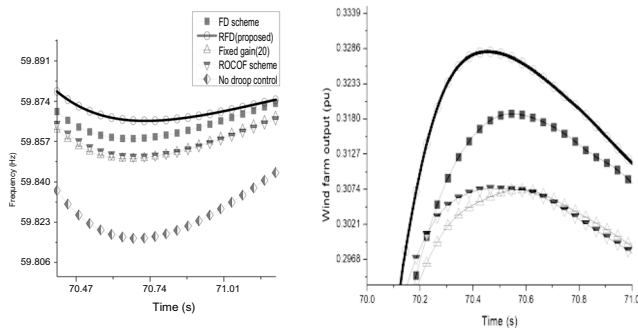

Fig. 8 Close-up versions of system frequency (left) and power output (right) for Case 3

from 8.1 to 16.3%. The order of the highest to lowest FN was identical to that of Case 1, as was the order of the fastest to slowest reaction time. These orders were the same for all cases; thus, for Cases 2 to 5, only the close-up versions of the system frequency and power output graphs were included to visualize the graph comparison for each droop control method.

The level of frequency deviation, however, was higher in Case 2 for all methods than in Case 1, and the RFD method had a 17.66% decrease in deviation compared to its value in Case 1. This is because higher wind penetration translates to more wind turbines in the system, implying that more individual units contribute to frequency regulation through droop control, thereby improving FN.

The difference in FN improvement between the RFD and other droop control methods also increased, with the FN improvement of RFD method being 3.64% greater than that of the FD method and 7.96% greater than that of the fixed droop method.

Similar to the FN value, all methods of droop control showed slightly slower reaction times in Case 2 than in Case 1, with the RFD method having a reaction time 20.69% slower in Case 2 than in Case 1. This is because the frequency deviation was smaller in Case 2 than in Case 1

because of the improved FN, and thus the droop value, being a function of the frequency deviation, increased at a slower rate, as did the output power.

5.1.3 Case 3: Wind Speed = 7 m/s, Penetration = 23.2%

The wind penetration in Case 3 is increased to 23.2% while maintaining the remaining system parameters. Similar to Case 2 compared to Case 1, Case 3 displayed a higher FN value owing to higher wind penetration, with the RFD method in Case 3 having a frequency deviation 29.83% smaller than that of Case 1.

The difference in FN improvement between the RFD method and the other droop control methods further increased as well, with the FN improvement of RFD method being 4.08% greater than that of the FD method and 8.67% greater than that of the fixed droop method.

A slower total reaction time was also observed owing to the improved FN, with the RFD method having a reaction time 44.83% slower in Case 3 than in Case 1.

5.1.4 Effects of Wind Speeds

In this section, the frequency support capability of droop control based on wind speed was analyzed. Because the kinetic energy of the WTG is determined by the wind speed, wind speed is an important factor in droop control. When operated in MPPT mode, the rotor speed changes based on the wind speed. When a frequency drop was present, a large PFR could be provided at a high rotor speed; however, a secondary frequency drop or wind turbine stalling problem could occur when a large PFR was provided at a low rotor speed [14, 20]. Therefore, it is important to improve FN without generating a second-order frequency droop at low wind speeds.

Additionally, unlike Cases 1–3, in Cases 4–5, the rotor speed changed because the wind speed was different. The $1/R_\omega$ ratio of the RFD droop control and rotor speed were analyzed to confirm the stability capability of the RFD droop control.

5.1.5 Case 4: Wind Speed = 6.5 m/s, Penetration = 23.2%

In Case 4, the FN improvement ability was in the following order: RFD, FD, ROCOF, fixed droop, and no-droop control. The FN improvement ability of the RFD droop control differed by 0.56% from that of the FD, which had the best FN improvement performance among the existing droop controls. There was a difference of 5.52% from the fixed droop control, which had a poor performance. Compared to Cases 1 to 3, the FN improvement ability of the RFD droop
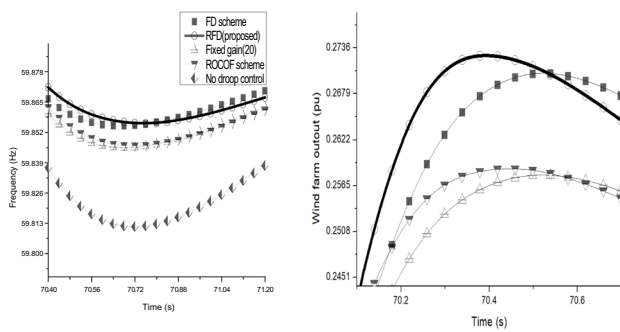
(a) Close-up versions of the system frequency (left) and power output (right)
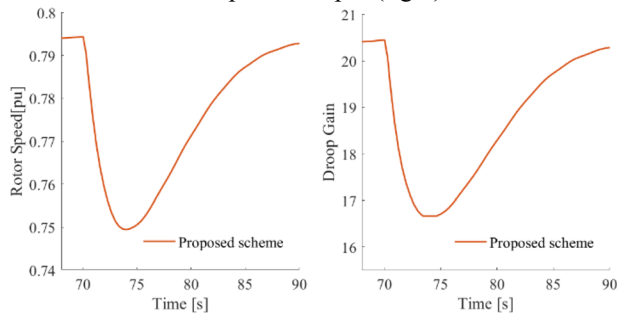
(b) Rotor speed (left) Droop gain (right)

Fig. 9 Simulation results for Case 4

(a) Close-up versions of the system frequency (left) and power output (right)

(b) Rotor speed (left) droop gain (right)

Fig. 10 Simulation results for Case 5

control in Case 4 was insignificant compared to other droop controls. This is because the rotor was operated at a low speed, as shown in.

Figure .9 b, thus the $1/R_\omega$ value changed, as shown in Fig. 9 b. This ability can effectively solve problems such as secondary frequency drop by limiting the PFR to too much at low wind speeds

The reaction time was 25% faster in RFD droop control than in FD. This indicates that RFD droop control supports the PFR faster.
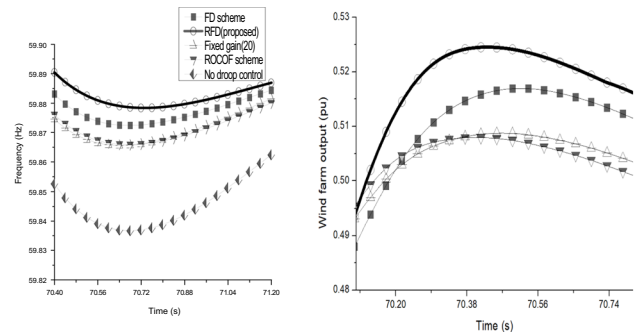
5.1.6 Case 5: Wind Speed = 8.5 m/s, Penetration = 23.2%

The wind speed set at 6.5 m/s in Case 4 changed to 8.5 m/s in Case 5 to observe the frequency support capability of droop control at high wind speeds.
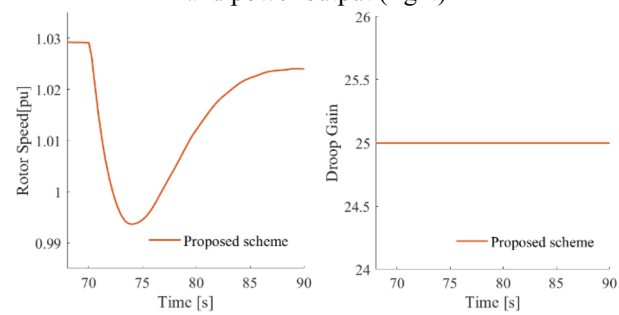
The wind speed increased, and the overall FN increased compared to that in Case 4. This is because the higher the wind speed, the more energy is available to support the initial frequency.

The FN improvement ability was high in the order of RFD, FD, ROCOF, Fixed, and no-droop control. The FN improvement ability of the RFD droop control differed by 3.64% from that of the FD droop control and 7.82% from that of the fixed droop control.

This is because the $1/R_\omega$ gain increased owing to the increased rotor speed, as shown in Fig. 10b. The gain

value $1/R_\omega$ of the RFD droop control of Case 5 is shown in Fig. 10b. Because the wind speed was high and the rotor speed rotated rapidly, $1/R_\omega$ had the maximum gain value, as shown in Fig. 10b.

The reaction time of the RFD droop control was 17.65% faster than that of the FD. A small difference was observed when compared to Case 4, which showed improved FN.

6 Conclusion

This study proposes a modified variable droop control method that can effectively improve the FN and achieve fast PFR at the initial point of the frequency drop. Other previous droop control strategies have utilized each of these advantages individually; as the ROCOF method has a quicker PFR reaction time, and the FD method has a higher FN improvement. Both the ROCOF and frequency deviation allowed the proposed RFD droop control strategy to attain both of these advantages. Further, by properly adjusting the gain based on the rotor speed, the secondary frequency drop that occurs when the wind speed is significantly low or high can be prevented.

The power system was designed by simulation, and the FN improvement ability of the RFD droop control was verified based on the wind penetration and wind speed. Consequently, when the wind penetration was increased, the RFD

method showed an improved FN and faster response compared to the existing method. Moreover, safe droop control was performed when the wind speed was low, and the FN improvement ability improved when the wind speed was high. Furthermore, the RFD droop control was composed of simple calculations; therefore, the mathematical calculations were not particularly complex. This can achieve a fast feedback system, which helps in more effective wind power operation. Therefore, the proposed RFD method is expected to contribute to the frequency stability of power systems and improve the penetration rate of wind power generation.

Future research should consider how to support the frequencies that wind turbines can support at low wind speeds. At low wind speeds, the ability of the wind power to control the droop is limited because the wind turbine has a small reserve power. Therefore, further research is required to ensure that the wind turbine can contribute to a stable power grid system, even at low wind speeds.

References

1. Rashid MH (2016) Electric Renewable Energy Systems. Academic Press, pp 60–77
2. Zerrahn A (2017) Wind power and externalities. Ecol Econ 141:245–260
3. Vargas SA, Esteves GRT, Maçaira PM, Bastos BQ, Oliveira FLC, Souza RC (2019) Wind power generation: a review and a research agenda. J Clean Prod 218:850–870
4. Oh B, Kim S, Lee D (2023) Wind power scenario synthesis with smoothing effect through spectral decomposition and its application to flexible resource adequacy. IEEE Trans Sustain Energy 14(2):777–789
5. Vidyanandan KV, Senroy N (2012) Primary frequency regulation by deloaded wind turbines using variable droop. IEEE Trans Power Syst 28(2):65–72
6. Singh, M., Muljadi, E., Jonkman, J., Gevorgian, V., Girsang, I., and Dhupia, J (2014), *Simulation for Wind Turbine Generators With Fast and Matlab-Simulink Modules*, NREL
7. Morren J, Hero de Haan SW, Kling WL, Ferreira JA (2006) Wind Turbines Emulating Inertia and Supporting Primary Frequency Control. IEEE Trans Power Syst 21(1):433–434
8. M Venkatasubramanian and K Tomsovic (2005), *The electrical engineering handbook*, Academic Press,.
9. Lalor G, Mullane A, O'Malley M (2005) Frequency control and wind trbine technologies. IEEE Trans Power Syst 20(4):1905–1913
10. Li J, Ma Y, Gang M, Feng X, Yan G, Guo G, Zhang T (2018) Optimal configuration of energy storage system coordinating wind turbine to participate power system primary frequency regulation. Energies 11(6):1396
11. Miao Lu, Wen J, Xie H, Yue C, Lee W-J (2015) Coordinated control strategy of wind turbine generator and energy storage equipment for frequency support. IEEE Trans Ind Appl 51(4):2732–2742
12. Wang H, Yang J, Chen Z, Ge W, Ma Y, Xing Z, Yang L (2018) Model predictive control of pmsg-based wind turbines for frequency regulation in an isolated grid. IEEE Trans Ind Appl 54(4):3077–3089
13. Kumar D, Pavitra Sharma HD, Mathur SB, Bansal RC (2020) Modified deloading strategy of wind turbine generators for primary frequency regulation in micro-grid. Technol Econ Smart Grids Sustain Energy 5(11):1–12
14. Yang D, Jin Z, Zheng T, Jin E (2021) An adaptive droop control strategy with smooth rotor speed recovery capability for type iii wind turbine generators. Int J Electr Power Energy Syst 135:107532
15. Panayiotis Moutis, Emmanouil Loukarakis, Stavros Papathanasiou and Nikos D. Hatziargyriou (2009), "Primary load-frequency control from pitch-controlled wind turbines," *in IEEE Bucharest PowerTech*, Bucharest, Romania,
16. Chavero Navarrete E, Trejo Perea M, Jáuregui Correa JC, Carrillo Serrano RV, Moreno GJR (2019) Expert control systems implemented in a pitch control of wind turbine: a review. IEEE Access 7:13241–13259
17. Van TL, Nguyen TH, Lee D-C (2015) Advanced pitch angle control based on fuzzy logic for variable-speed wind turbine systems. IEEE Trans Energy Conv 30(2):578–587
18. Fusheng Li, Ruisheng Li, Fengquan Z (2015) Microgrid technology and engineering application. Elsevier, pp 11–27
19. Mehrizi-Sani A (2017) Microgrids. Elsevier, pp 43–62
20. Yang D, Zheng T, Jin E, Zhang X, Hua L (2021) Frequency control scheme with dynamic droop characteristics of a DFIG for mitigating the frequency fluctuations. Int Trans Electr Energy Syst 31(11):e13044
21. Yien Xu, Chen P, Zhang X, Yang D (2021) An improved droop control scheme of a doubly-fed induction generator for various disturbances. Energies 14(23):7980
22. Li P, Hu W, Hu R, Huang Q, Yao J, Chen Z (2015) Strategy for wind power plant contribution to frequency control under variable wind speed. Renew energy 130:1226–1236
23. Naidu NKS, Singh B (2017) Grid-Interfaced, DFIG-based variable speed wind energy conversion system with power smoothening. IEEE Trans Sustain Energy 8(1):51–58
24. Arani MFM, Mohamed YA-RI (2017) Dynamic droop control for wind turbines participating in primary frequency regulation in microgrids. IEEE Trans Smart Grid 9(6):5742–5751
25. Garmroodi M, Verbič G, Hill DJ (2017) Frequency support from wind turbine generators with a time-variable droop characteristic. IEEE Trans Sustain Energy 9(2):676–684
26. Kang M et al (2016) Frequency control support of a doubly-fed induction generator based on the torque limit. IEEE Trans Power Syst 31(6):4575–4583
27. Hwang M, Muljadi E, Park J-W, Sørensen P, Kang YC (2016) Dynamic droop-based inertial control of a doubly-fed induction generator. IEEE Trans Sustain Energy 7(3):924–933
28. Kim Y, Kang M, Muljadi E, Park J-W, Kang YC (2016) Power smoothing of a variable-speed wind turbine generator in association with the rotor speed-dependent gain. IEEE Trans Sustain Energy 8(3):990–999
29. Pradhan C, Bhende CN (2016) Frequency sensitivity analysis of load damping coefficient in wind farm-integrated power system. IEEE Tran. Power Syst 32(2):1016–1029
30. Yang D, Kim J, Kang YC, Muljadi E, Zhang N, Hong J, Song S-H, Zheng T (2018) Temporary frequency support of a DFIG for high wind power penetration. IEEE Trans Power Syst 33(3):3428–3437

Joseph Shin received B.S. degree in mechanical & Control engineering from Handong Global university. His research interests are wind generation and robotic control.

Suhyeon Han received B.S. degree in mechanical & Control engineering from Handong Global university. Her research interests are wind generation.

Sejin Lee received B.S. degree in mechanical & Control engineering from Handong Global university. His research interests are wind generation and power electronics.

Youngsung Kwon received B.S. degree in Electrical Engineering from Soongsil University, Seoul, South Korea in 2009, and his M.S.E. and Ph.D. degree in Electrical and Computer Engineering from the University of Texas at Austin in 2012 and 2015, respectively. From 2015 to 2018, he was with LG Electronics of South Korea, designing and developing electric vehicle charging system. Since 2018, he has been an assistant professor at the Handong Global University of South Korea and his current research interests include power electronic system, renewable and alternative energy, and microgrids.